RESEARCH PAPER

PCCP
www.rsc.org/pccp

High resolution FTIR spectroscopy of the ν_1 band of NSCl†

Evan G. Robertson,* Christopher D. Thompson, Sebastian Lucie and Don McNaughton

School of Chemistry, Monash University, PO Box 23, Victoria, 3800, Australia.
E-mail: evan.robertson@sci.monash.edu.au; Fax: +61 3 9905 4597; Tel: +61 3 99054566

Received 20th October 2004, Accepted 1st December 2004
First published as an Advance Article on the web 11th January 2005

The highly reactive molecule thiazyl chloride (NSCl) prepared by pyrolysis of $S_3N_2Cl_2$ at 70 °C was measured by high resolution (0.003 cm^{-1}) FTIR spectroscopy in the mid-IR region. Detailed analyses of ν_1, the hybrid a/b-type band at 1325.6 cm^{-1}, led to assignment of 6275 and 3836 lines, respectively, for the $^{14}N^{32}S^{35}Cl$ and $^{14}N^{32}S^{37}Cl$ isotopomers. Fitting to Watson's *A*-reduced Hamiltonian led to the first rovibrational constants for the ν_1 mode along with an improved set of ground state constants including centrifugal distortion beyond the quartic level.

1. Introduction

Thiazyl chloride (NSCl) is a reactive gaseous species that coexists in equilibrium with its trimer at room temperature. The low resolution IR spectrum was first measured in the gas phase by Müller *et al.*,[1,2] who deduced a bent molecular structure of C_s symmetry with the sulfur atom in the centre. Six isotopomers, including some with ^{37}Cl, ^{15}N or ^{34}S atoms, were examined in a matrix IR study[3] and low temperature IR spectra of solid films have also been measured recently.[4] Microwave spectroscopy data was used to determine the bond lengths and angles of NSCl through isotopic substitution,[5] and to determine the dipole moment and centrifugal distortion parameters.[6] The geometry ascertained by electron diffraction is consistent with the microwave results.[7] Several empirically determined harmonic force fields have been reported[1–3,5,6,8] along with anharmonic force fields computed *ab initio* at the Hartree–Fock level.[9,10] High level *ab initio* molecular orbital calculations have been used to compute anharmonic vibrational wavenumber values,[11] and to show that thiazyl chloride is around 22 kcal mol^{-1} more stable than thionitrosyl chloride ion, ClNS.[12] NSCl has also been used as a precursor in the attempted gas-phase pyrolytic generation of NSCN[13] and NSSCN.[14] However, thorough examination of the spectra suggested that bands at 2224 and 1374 cm^{-1} assigned to NSCN were actually those of N_2O and SO_2. Likewise, the 'NSSCN' bands at 2060, 1365 and 712.6 cm^{-1} were reassigned to OCS, SO_2 and HCN.[15] High resolution IR studies have helped reveal structural information concerning similarly reactive triatomic molecules, such as NSF,[16] OPCl[17] and OPF.[18] In the present study, we generate NSCl(g), measure for the first time its high resolution IR spectrum and analyse the ν_1 band at 1325.6 cm^{-1}. We also report the results of (unsuccessful) pyrolysis experiments aimed at the production of NSCN from NSCl vapour.

2. Experimental

A. Preparation of thiodiazyl dichloride ($S_3N_2Cl_2$)

The following preparation was adapted from the syntheses of Logan and Jolly[19] and Gillespie and Passmore.[20] The synthesis must be carried out at the rear of the fumehood where the air flow is consistent and all glassware baked to total dryness. Anhydrous ammonium chloride (NH_4Cl, BDH), disulfur dichloride (S_2Cl_2, Aldrich) and powdered sulfur (S_8, BDH) are placed in a two-necked 500 ml round-bottom flask with the stoichiometric ratio [3 : 1 : 0.05]. A 50 cm air condenser is positioned vertically above the flask with the second neck containing a nitrogen line for purging water vapour from the system during preparation.

The flask is lowered into a heating mantle and brought to reflux (S_2Cl_2 bp = 136 °C) ensuring a condensation level about one third from the bottom of the air condenser. The first signs of product appear after 30 min. Aluminium foil is wrapped about the exposed sections to minimise the draught, as fluctuation in the condensation level results in the orange-brown crystalline product being washed back into the reaction flask. The reaction can be considered complete after 4–5 h. The moisture sensitive crystals are collected in a dry-bag with a yield of ≈5%. The micro-Raman spectrum of this product has bands at 1015, 934, 728, 579, 405, 385, 368 and 349 cm^{-1}, confirming its identity as $S_3N_2Cl_2$.[21]

B. Preparation of thiazyl chloride (NSCl)

While previous preparations of NSCl involved the heating of the trimeric $(NSCl)_3$ (prepared by passing chlorine gas over thiodiazyl dichloride ($S_3N_2Cl_2$) and also generating SCl_2), in this case only small pressures were required, and a less hazardous method was used. Pyrolysis of $S_3N_2Cl_2$ at 70 °C generated sufficient vapour pressure of NSCl to pass through a White cell for high resolution FTIR analysis. A flow through technique is required to minimise the build-up of by-products that form rapidly by hydrolysis with trace moisture:

$$NSCl + H_2O \rightarrow HNSO + HCl$$

$$HNSO + H_2O \rightarrow NH_3 + SO_2$$

Pressures were maintained at *ca.* 30 Pa. The ≈53 cm White cell is used with eight passes to give a total optical path length of 4.24 m. The cell, which operates at room temperature, is coupled to a Bruker 120HR interferometer equipped with a Globar as an IR source and an InSb/HgCdTe sandwich detector to measure spectra above and below 1800 cm^{-1}, respectively. High resolution spectra were recorded with notional resolution of 0.003 cm^{-1} and the 4P (4 point)

† Electronic supplementary information (ESI) available: Output files from the fits of the experimental sets of $^{14}N^{32}S^{35}Cl$ and $^{14}N^{32}S^{37}Cl$ data using the program SPFIT written by Pickett.[24] See http://www.rsc.org/suppdata/cp/b4/b416215c/

DOI: 10.1039/b416215c

apodisation function was used to minimise linewidths. A long-wave-pass optical filter (1% transmission at 1550 cm^{-1}) was used to restrict incident radiation. A total of nearly 200 scans were recorded at high resolution. High resolution scans of the by-products SO_2 and HNSO were also recorded for the purpose of spectral subtraction.

C. Pyrolysis of NSCl over AgCN

In a two step flow pyrolysis procedure, NSCl vapour generated by heating $S_3N_2Cl_2$ to 60 °C was passed over AgCN(s). A second furnace heated the AgCN to temperatures in the range 160–370 °C. Cell pressures were maintained in the range 10–80 Pa by controlling the rate at which the sample cell was pumped. This corresponded to a cell residence time of *ca.* 1 min. Spectra were measured with moderate resolution (0.019–0.125 cm^{-1}) over the range 650–4000 cm^{-1}.

3. Results

A. NSCl analysis

ν_1 is the NS stretch mode of NSCl. Its vibrational frequency is consistent with a bond order $N_{NS} > 2$.[1] The high resolution (0.003 cm^{-1}) IR spectrum of ν_1 shown in Fig. 1 reveals a predominantly a-type band. The water lines that are evident around 1350–1400 cm^{-1} are from trace moisture in the interferometer compartment. Their positions were used to calibrate the spectra by comparison with measured line positions from the HITRAN database.[22] In common with earlier low resolution studies,[1,14] we also observe bands associated with HNSO and SO_2 from hydrolysis with trace quantities of water. The half-life for conversion of NSCl to HNSO was observed to be a few minutes when the pyrolysis products were isolated in the cell and monitored by rapid survey scans. Using static conditions, high resolution spectra of HNSO and SO_2 in the absence of NSCl were measured for the purpose of spectral subtraction. Fig. 2 illustrates how this aided the spectral analysis. The ν_1 band of NSCl has a weak b-type component that is swamped by a-type lines within 20 cm^{-1} of the band centre, but emerges in the wings. However, the b-type transitions (simulated in Fig. 2e) only become evident once the SO_2 contribution is removed to give the resultant spectrum shown in Fig. 2c. Subtraction of the SO_2 band from the R-branch and the HNSO band from the P-branch allowed assignment of NSCl transitions over a wide range, 1379–1278 cm^{-1}.

Spectral assignments were facilitated by the software program MACLOOMIS, which displays peak lists in Loomis–Wood format[23] to enable series of regularly spaced lines to be identified. The most abundant $^{14}N^{32}S^{35}Cl$ isotopomer was examined first. Initially, around 3300 a-type transitions and 1000 b-type transitions were assigned, with J quantum numbers up to 98 and K_a up to 21. Peaks that appeared to be blended in the Loomis–Wood display were omitted. The IR transitions were given an experimental uncertainty of 0.0003 cm^{-1} for the least squares fits described below. Published microwave transitions involving the ground state[6] were also included with an uncertainty of 0.1 MHz.

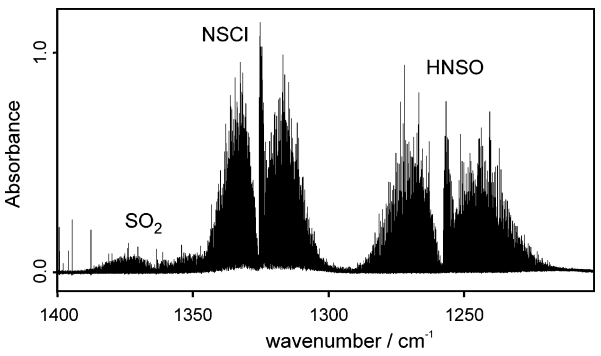

Fig. 1 Overview spectrum in the 1200–1400 cm^{-1} region showing bands of NSCl and the by-products SO_2 and HNSO.

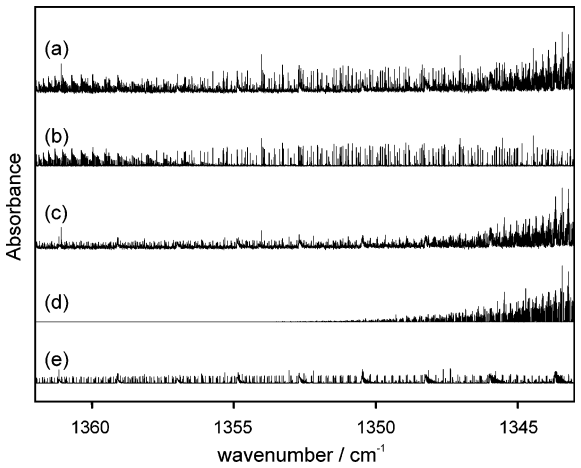

Fig. 2 Spectra in the region where NSCl and SO_2 bands overlap: (a) experimental spectrum of NSCl with SO_2 present, (b) spectrum of SO_2 without NSCl, (c) NSCl spectrum resulting from subtraction of SO_2 spectrum. (d) Simulation of the a-type component and (e) the b-type component of the $^{14}N^{32}S^{35}Cl$ fundamental band.

The combined data set was fitted to Watson's A-reduced Hamiltonian using the program SPFIT written by Pickett.[24] A satisfactory fit with rms error of 0.000 33 cm^{-1} was obtained by including all quartic centrifugal distortion constants and some higher order diagonal terms.

Analysing the ν_1 band of the less abundant $^{14}N^{32}S^{37}Cl$ isotopomer using the raw experimental spectrum is more difficult because it is obscured by stronger, overlapping $^{14}N^{32}S^{35}Cl$ transitions. In these circumstances, the Spectral Analysis by Subtraction of Simulated Intensities (SASSI) approach that we developed[25,26] is of considerable help. A simulated band system is subtracted from the experimental spectrum over the entire region, as opposed to the routine subtraction of experimental data or line by line deconvolution of overlapping features in high-resolution spectra. This procedure has been shown to be a useful global approach to revealing minor components of spectra including minor isotopomers and hot-bands.

To apply the SASSI approach, line positions and intensities were generated with Pickett's SPCAT program[24] and convolved using a Gaussian lineshape function to produce a spectrum in the range 1270–1390 cm^{-1}. The points were chosen to precisely coincide with those of the experimental spectra, separated by 0.000 38 cm^{-1}. The notional resolution is 0.0030 cm^{-1}, but experimental spectra are Fourier transformed with a zero fill factor of 2 and the region of interest subsequently post zero filled by a further factor of 4 to obtain better lineshapes. The optimal value for the a/b hybrid ratio was found to be 11 ± 1, and the most suitable full width-half maximum linewidth 0.0030 cm^{-1}. A portion of the simulated $^{14}N^{32}S^{35}Cl$ band is shown in Fig. 3b. It is evident that the raw experimental spectrum shown in Fig. 3a is dominated by the $^{14}N^{32}S^{35}Cl$ fundamental. With this component subtracted, the resultant spectrum of Fig. 3c shows the emergence of weaker, underlying features including those associated with the $^{14}N^{32}S^{37}Cl$ fundamental. Fig. 3d is a simulation of the $^{14}N^{32}S^{37}Cl$ band based on data derived from this work (and described below).

Examination of the resultant spectrum by Loomis–Wood plots led to assignment of over 2200 transitions of the $^{14}N^{32}S^{37}Cl$ fundamental, with the quantum numbers up to $J_{max} = 89$, $K_{a\ max} = 15$. A simultaneous fit to the IR data and the microwave transitions from ref. 5 yielded a preliminary set of constants.

In a further refinement of the SASSI procedure, a series of simulations were generated with all the components present

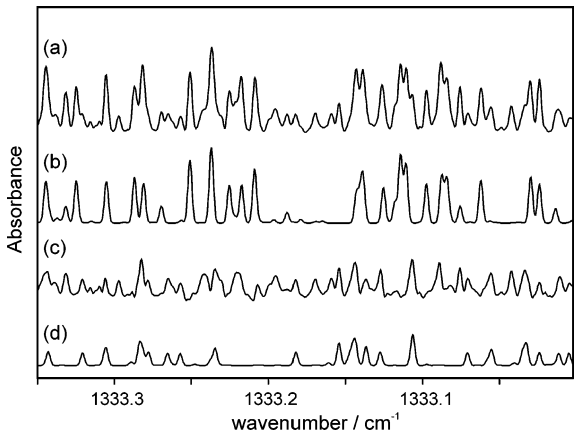

Fig. 3 (a) Expanded experimental spectrum of the ν_1 band of NSCl, together with (b) a simulation of the $^{14}N^{32}S^{35}Cl$ fundamental band, (c) the resultant, subtracted spectrum and (d) a simulation of the $^{14}N^{32}S^{37}Cl$ fundamental band. Simulations are based on spectroscopic parameters in Table 1, with $T_{rot} = 298$ K, a/b hybrid ratio 11 and Gaussian full width half-maximum linewidth 0.0030 cm^{-1}.

except selected transitions of one band in a limited K_a range. In this way, weaker transitions associated with high J and K_a quantum numbers stand out in the resultant spectra. As a consequence, the number of the transitions assigned to the $^{14}N^{32}S^{35}Cl$ fundamental increased to 6275 and the maximum K_a to 23. Similarly, 1580 more transitions of $^{14}N^{32}S^{37}Cl$ transitions were assigned with the maximum K_a now 18.

The fits to the enlarged sets of $^{14}N^{32}S^{35}Cl$ and $^{14}N^{32}S^{37}Cl$ data are summarized in Table 1; full details, including lists of transitions, are available as ESI.† The diagonal, sextic centrifugal distortion constants were included in addition to L_K. The quality of the fits is excellent. The rms error is just 0.000 27 cm^{-1} for IR transitions of $^{14}N^{32}S^{35}Cl$ and 0.000 33 cm^{-1} for $^{14}N^{32}S^{37}Cl$. The ground state rotational constants of $^{14}N^{32}S^{35}Cl$ are very similar to those from the analysis of Mitzumo *et al.* in which centrifugal distortion was treated to the quartic level.[6] The discrepancies in A and C are within the experimental error. However, the $^{14}N^{32}S^{37}Cl$ constants are somewhat different from those reported by Beppu *et al.*[5] For example, the A constant is larger by 1.6 MHz. The inconsistency arises chiefly from the use of a rigid-rotor Hamiltonian in the earlier study because of the restricted data set of that study. The ν_1 constants of Table 1 are the first experimental values to be reported. Vibrational–rotational constants, α, for ν_2 and ν_3 are known from microwave vibrational satellite data,[27] so the equilibrium rotational constants for $^{14}N^{32}S^{35}Cl$ can now be evaluated: $A_e = 41\,468.892$ MHz, $B_e = 4127.7900$ MHz, $C_e = 3754.3261$ MHz. The small inertial defect, $\Delta_e = -0.0078$ u Å^2, is consistent with a planar molecule.

Table 2 compares fitted quartic centrifugal distortion constants with those calculated from the empirically derived force field of Müller *et al.*[2] The two sets of ground state constants for $^{14}N^{32}S^{35}Cl$ are within 6%. The proportional changes upon isotopic substitution of ^{37}Cl for ^{35}Cl also compare favourably, with the exception of δ_K which is the least well determined quartic parameter.

B. Pyrolysis of NSCl over AgCN

IR spectra were measured for a range of pyrolysis temperatures, beginning at 160 °C, the temperature used in the original pyrolysis paper.[13] NSCl was present under all conditions (observed *via* the ν_1 band at 1325.6 cm^{-1} and its previously unreported overtone at 2634 cm^{-1}). N_2O and SO_2 were observed among the products. The most intense bands of N_2O and SO_2 at 2224 cm^{-1} and 1374 cm^{-1}, respectively were mistakenly assigned to NSCN in the earlier work. With improved spectral resolution in the present study, the rotational structure in these bands is sufficiently resolved to

Table 1 Fitted spectroscopic constants for the ν_1 fundamentals of NSCl in the A-reduced I_r representation

	$^{14}N^{32}S^{35}Cl$	$^{14}N^{32}S^{37}Cl$
ν_0/cm^{-1}	1325.573 074(14)[a]	1325.572 564(22)
A''/MHz	41 723.4365(246)	41 624.719(41)
B''/MHz	4114.243 94(258)	3997.4064(77)
C''/MHz	3738.583 08(242)	3641.0583(62)
Δ_J''/MHz	$2.635\,66(91) \times 10^{-03}$	$2.501\,87(103) \times 10^{-03}$
Δ_{JK}''/MHz	−0.039 7888(255)	−0.038 844(85)
Δ_K''/MHz	1.665 85(33)	1.654 74(86)
δ_J''/MHz	$3.627\,78(160) \times 10^{-04}$	$3.3728(35) \times 10^{-04}$
δ_K''/MHz	0.018 390(177)	0.018 390(294)
H_J''/MHz	$6.98(64) \times 10^{-10}$ [b]	6.98×10^{-10} [c]
H_{JK}''/MHz	$5.130(216) \times 10^{-08}$	$4.72(64) \times 10^{-08}$
H_{KJ}''/MHz	$-9.987(55) \times 10^{-06}$	$-1.0867(267) \times 10^{-05}$
H_K''/MHz	$2.8492(142) \times 10^{-04}$	$2.9964(294) \times 10^{-04}$
L_K''/MHz	$5.612(175) \times 10^{-08}$ [b]	$5.612(175) \times 10^{-08}$ [c]
A'/MHz	41 403.7555(259)	41 304.876(45)
B'/MHz	4113.241 83(264)	3996.5222(77)
C'/MHz	3735.327 03(248)	3638.0062(63)
Δ_J'/MHz	$2.645\,89(91) \times 10^{-03}$	$2.511\,54(102) \times 10^{-03}$
Δ_{JK}'/MHz	−0.040 0651(260)	−0.039 118(85)
Δ_K'/MHz	1.649 02(34)	1.638 02(89)
δ_J'/MHz	$3.671\,11(159) \times 10^{-04}$	$3.4140(35) \times 10^{-04}$
δ_K'/MHz	0.018 384(173)	0.018 322(287)
H_J'/MHz	$6.98(64) \times 10^{-10}$ [b]	$6.98(64) \times 10^{-10}$ [c]
H_{JK}'/MHz	$5.131(217) \times 10^{-08}$	$4.63(64) \times 10^{-08}$
H_{KJ}'/MHz	$-9.949(56) \times 10^{-06}$	$-1.0847(267) \times 10^{-05}$
H_K'/MHz	$2.8164(143) \times 10^{-04}$	$2.9675(301) \times 10^{-04}$
L_K'/MHz	$5.612(175) \times 10^{-08}$ [b]	$5.612(175) \times 10^{-08}$ [c]
Δ''/u Å^2 [d]	0.2303 ± 1	0.2320 ± 3
Δ'/u Å^2 [d]	0.2247 ± 1	0.2264 ± 3
J max	99	95
K_a max	23	18
No. a-type transitions	5211	3600
No. b-type transitions	1064	236
rms error (IR)/cm^{-1}	0.000 273	0.000 326
No. transitions (MW)	26[e]	11[f]
rms (MW)/MHz	0.25	0.18

[a] Numbers in parentheses are 1 standard deviation according to the least squares fit in units of the least significant figure. [b] Constraint $H_J' = H_J''$, $L_K' = L_K''$. [c] Fixed to corresponding $^{14}N^{32}S^{35}Cl$ value. [d] $\Delta = I_c - I_a - I_b$ [e] From ref. 6. $5_{1,4} \leftarrow 5_{0,5}$ and $10_{2,9} \leftarrow 11_{1,10}$ were omitted due to unacceptably large residuals (−0.83 MHz and 1.18 MHz, respectively). The observed frequency for $12_{2,10} \leftarrow 13_{1,13}$ was set to 31601.97 MHz, correcting the typographical error in ref. 6. [f] From ref. 5, with $1_{1,1} \leftarrow 2_{0,2}$ omitted due to residual of −1.74 MHz.

Table 2 Ground state centrifugal distortion constants in the A-reduced I_r representation from experimental fits and calculated from force field set II of ref. 2

	$^{14}N^{32}S^{35}Cl$		Change upon ^{37}Cl substitution	
	Exp.	Force field	Exp.	Force field
Δ_J/kHz	2.636	2.699	−5.08%	−5.29%
Δ_{JK}/kHz	−39.79	−37.42	−2.37%	−3.32%
Δ_K/kHz	1666	1604	−0.67%	−0.95%
δ_J/kHz	0.3628	0.3692	−7.03%	−7.74%
δ_K/kHz	18.39	17.33	0.00%	−4.23%

confirm unambiguously their identity. Among the other products observed were CS_2, CO_2, HCN, ClCN, NCCN, OCS, HNCO, HNSO and HCl. According to appropriately scaled B3LYP/aug-cc-pVTZ predictions, the NSCN bands are expected at 2143 and 1336 cm^{-1}, with intensities 67 and 13 km mol^{-1}, respectively.[15] No evidence was found for these bands in our spectra. The furnace was not heated beyond 370 °C because AgCN decomposes at 320 °C. Spectra measured at and above 325 °C showed depletion of the cyano containing species NCCN and HCN.

4. Discussion and conclusions

The resultant spectrum of Fig. 3c shows additional peaks that are not present in the simulated fundamental bands of $^{14}N^{32}S^{35}Cl$ and $^{14}N^{32}S^{37}Cl$. These arise chiefly from hot-bands, associated with excitation in the ν_3 (272 cm^{-1}) and ν_2 (415 cm^{-1})^2 vibrational modes. At 298 K the vibrational partition function is *ca*. 1.59, so 37% of molecules will exist in excited vibrational states, including 17% in $v_3 = 1$ and 8.5% in $v_2 = 1$. It is feasible to proceed further with the analysis through the Spectral Analysis by Subtraction of Simulated Intensities (SASSI) approach, and this will be subject of a future paper. In the present situation, the SASSI method has helped in two ways. Firstly, it has helped assignment of features associated with the less abundant $^{14}N^{32}S^{37}Cl$ isotopomer by removing the contribution from the $^{14}N^{32}S^{35}Cl$ fundamental without the need for costly isotopically purified chemicals. Secondly, it has helped reveal weaker transitions of high quantum number by selective subtraction, *i.e*. transitions associated with certain quantum numbers are excluded from the simulation. This refinement of SASSI was used in a limited way with the ν_3 band of $CHClF_2$,[28] but has not been described before.

Finally, it appears that pyrolytic production of NSCN by passage of NSCl over AgCN is not viable. The bands at 2224 and 1374 cm^{-1}, previously assigned to NSCN, were shown conclusively to belong to N_2O and SO_2. Either NSCN is not produced at all, or it reacts extremely rapidly and consequently has a concentration too low to be detected. Alternative methods must be sought if NSCN is to be produced and studied by gas phase IR spectroscopy.

Acknowledgements

The authors gratefully acknowledge financial support from the Australian Research Council and from Monash University in the form of a Logan Fellowship (EGR) and a Special Dean's Faculty of Science Postgraduate Scholarship (CDT).

References

1 A. Müller, G. Nagarajan, O. Glemser, S. F. Cyvin and J. Wegener, *Spectrochim. Acta*, 1967, **23A**, 2883.
2 A. Müller, N. Mohan, S. J. Cyvin, N. Weinstock and O. Glemser, *J. Mol. Spectrosc*., 1976, **59**, 161.
3 S. C. Peake and A. J. Downs, *J. Chem. Soc., Dalton Trans*., 1974, 859.
4 W. C. Emken, K. W. Hedberg and J. C. Decius, *Spectrochim. Acta*, 1997, **53A**, 207.
5 T. Beppu, E. Hirota and Y. Morino, *J. Mol. Spectrosc*., 1970, **36**, 386.
6 S. Mizumoto, J. Izumi, T. Beppu and E. Hirota, *Bull. Chem. Soc. Jpn*., 1972, **45**, 786.
7 W. C. Emken and K. Hedberg, *J. Chem. Phys*., 1973, **58**, 2195.
8 V. Sankaran, *Discovery Innovation*, 1992, **4**, 45.
9 R. Cervellati, D. G. Lister and P. Palmieri, *THEOCHEM*, 1984, **17**, 321.
10 G. L. Bendazzoli, G. Cazzoli, C. Degli Esposti, G. Fano, F. Ortolani and P. Palmieri, *J. Chem. Phys*., 1986, **84**, 5351.
11 D. Duflot, N. Chabert, J.-P. Flament, J.-M. Robbe, I. C. Walker, J. H. Cameron, A. Giuliani, M.-J. Hubin-Franksin and J. Delwiche, *Chem. Phys*., 2003, **288**, 95.
12 P. A. Denis, O. N. Ventura, H. T. Mai and M. T. Nguyen, *J. Phys. Chem. A*, 2004, **108**, 5073.
13 A. W. Allaf and R. J. Suffolk, *J. Chem. Res*., 1994, **1**, 186.
14 Z. Ajji, D. Y. Naima, M. N. Odeh and A. W. Allaf, *Spectrochim. Acta*, 1999, **55A**, 1753.
15 E. G. Robertson and D. McNaughton, *J. Phys. Chem. A*, 2003, **107**, 642.
16 U. Magg, J. Lindenmayer and H. Jones, *J. Mol. Spectrosc*., 1987, **126**, 270.
17 I. S. Bell, P. A. Hamilton and P. B. Davies, *J. Mol. Spectrosc*., 2000, **200**, 287.
18 H. Beckers, H. Bürger, P. Paplewski, M. Bogey, J. Demaison, P. Dréan, A. Walters, J. Breidung and W. Theil, *Phys. Chem. Chem. Phys*., 2001, **3**, 4247.
19 N. Logan and W. L. Jolly, *Inorg. Chem*., 1965, **4**, 1508.
20 R. J. Gillespie and J. Passmore, *Chem. Br*., 1972, **8**, 475.
21 I. Nevitt, H. S. Rzepa and J. D. Woollins, *Spectrochim. Acta*, 1989, **45A**, 367.
22 L. S. Rothman, C. P. Rinsland, A. Goldman, S. T. Massie, D. P. Edwards, J.-M. Flaud, A. Perrin, C. Camy-Peyret, V. Dana, J.-Y. Mandin, J. Schroeder, A. McCann, R. R. Gamache, R. B. Wattson, K. Yoshino, K. V. Chance, K. W. Jucks, L. R. Brown, V. Nemtchinov and P. J. Varansasi, *J. Quant. Spectrosc. Radiat. Transfer*, 1998, **60**, 665–710.
23 D. McNaughton, D. McGilvery and F. Shanks, *J. Mol. Spectrosc*., 1991, **149**, 458.
24 H. M. Pickett, *J. Mol. Spectrosc*., 1991, **148**, 371.
25 C. D. Thompson, E. G. Robertson and D. McNaughton, *Phys. Chem. Chem. Phys*., 2003, **5**, 1996.
26 D. McNaughton, I. Aleksic, D. R. T. Appadoo, C. D. Thompson and E. G. Robertson, *Vib. Spectrosc*., 2004, **36**, 123.
27 α_2 and α_3 computed using the rigid rotor rotational constants for ν_2, ν_3 and the ground state from ref. 5.
28 C. D. Thompson, E. G. Robertson and D. McNaughton, *Mol. Phys*., 2004, **102**, 1687.

